JACS
JOURNAL OF THE AMERICAN CHEMICAL SOCIETY
Article
pubs.acs.org/JACS

Crucial Role of Protein Flexibility in Formation of a Stable Reaction Transition State in an α-Amylase Catalysis

Takahiro Kosugi and Shigehiko Hayashi*

Department of Chemistry, Graduate School of Science, Kyoto University, Kyoto 606-8502, Japan

Supporting Information

ABSTRACT: Conformational flexibility of proteins provides enzymes with high catalytic activity. Although the conformational flexibility is known to be pivotal for the ligand binding and release, its role in the chemical reaction process of the reactive substrate remains unclear. We determined a transition state of an enzymatic reaction in a psychrophilic α-amylase by a hybrid molecular simulation that allows one to identify the optimal chemical state in an extensive conformational ensemble of protein. The molecular simulation uncovered that formation of the reaction transition state accompanies a large and slow movement of a loop adjacent to the catalytic site. Free energy calculations revealed that, although catalytic electrostatic potentials on the reactive moiety are formed by local and fast reorganization around the catalytic site, reorganization of the large and slow movement of the loop significantly contributes to reduction of the free energy barrier by stabilizing the local reorganization.

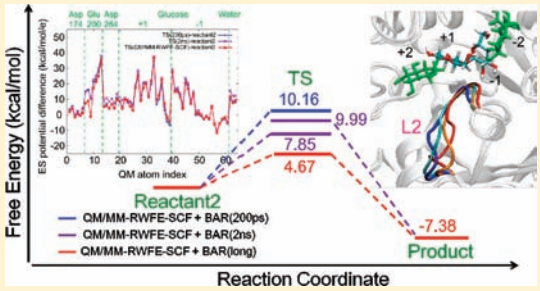

INTRODUCTION

Enzymes as biological catalysts are furnished with high catalytic activity. As well as chemical catalysts, substrate binding pockets of protein preorganize to stabilize chemically active states of the substrates, such as reaction transition states, by specific and selective molecular interactions between them. In addition to the preorganization, crucial roles of protein flexibility and plasticity, which differentiate enzymes from chemical catalysts, have long been recognized. Proteins exhibit large and slow dynamic fluctuation between conformational substates through which their structures are altered upon the substrate bindings and releases to accommodate well the substrates and to form the preorganized structure of the binding pocket.[1−5]

However, significance of the protein flexibility for catalytic reaction processes in the binding pockets, which involve only local geometric changes of the substrates, has been under debate.[6−9] Since the reaction transition state forms only transiently, direct and simultaneous detection of the correlation between the chemical reaction and the slow fluctuation of protein through experiments is rather difficult. On the other hand, molecular dynamics (MD) simulations with combined quantum mechanical/molecular mechanical (QM/MM) techniques[10−14] allow one to identify the reaction transition states in the binding pockets and to examine the catalytic preorganization as well as protein motion coupled with the catalytic reactions.[6,8,15] However, QM/MM MD simulations have been limited to follow protein dynamics on a time scale less than a nanosecond due to huge computational costs of the QM calculations included, and thus a role of the large and slow nonlinear protein conformational fluctuation on nanoseconds and longer time scales in chemical reaction processes remains unclear.

Here we report a QM/MM simulation study that unveils large and slow conformational changes on the tens of nanoseconds time scale upon formation of a transition state of an enzymatic reaction of an α-amylase from the Antarctic bacterium *Pseudoalteromonas haloplanktis*. The α-amylase studied is an endoacting enzyme for catalysis of hydrolysis of polysaccharides by cleaving internal α-1,4-glycosidic bonds. Despite a relatively simple reaction involved, enzymatic activity for the reaction exhibits peculiar temperature dependence. The α-amylase from the Antarctic bacterium is known to be psychrophilic, i.e., significantly more active at low temperature compared to homologous mesophilic ones in spite of close similarity of the amino acids constituting the active sites. Naturally, it is considered that the temperature dependence of the catalytic activity of those enzymes is related to structural flexibility of the enzymes, and in fact those enzymes have been observed to show characteristic features of structural flexibility and thermodynamic properties.[16−22] Thus, it is expected that the structural flexibility gives a significant contribution to the reaction catalysis in the enzymes, and elucidation of the molecular mechanism provides a conceptual insight into a role of protein flexibility in enzymatic catalysis, which has been under debate recently as described above.

We determined the free energetically optimal reaction transition state by the QM/MM reweighting free energy self-consistent field (QM/MM-RWFE-SCF) method.[23] The method developed recently features a remarkably high computational efficiency and was demonstrated to be capable of determining free energetically optimal geometries of the

Received: December 27, 2011
Published: April 2, 2012

   dx.doi.org/10.1021/ja212117m | J. Am. Chem. Soc. 2012, 134, 7045−7055

reactive substrate moiety in the reactant and product states on free energy surface that involves extensive conformational changes of protein on a nearly submicro second time scale.[23] In this study, we focused on a chemical reaction step of the glycosidic bond dissociation shown in Figure 1 and investigated protein reorganization involving large conformational changes upon the formation of the reaction transition state, energetics of the chemical reaction, and relaxation of the protein reorganization, which shed light on molecular mechanism of the reaction kinetics associated with the protein reorganization originating from the protein's flexibility. Through calculations of the reaction free energy barrier by MD simulations for nearly half a microsecond, the large and slow protein conformational changes were found to stabilize significantly the reaction transition state, and thus to contribute energetically to enhancement of the kinetic rate.

THEORETICAL BACKGROUND

QM/MM Geometry Optimization on Free Energy Surface. The QM/MM-RWFE-SCF method[23] combines a QM/MM free energy optimization method based on a mean field approximation developed by Yamamoto[24] with a reweighting update scheme for statistical ensemble of protein conformation introduced by Yang and co-workers.[25] A description of basic formulation of the method is presented in Supporting Information.

Briefly, the method determines the optimal electronic wave function and geometry of the reaction substrate molecules treated quantum mechanically (QM) in a protein mean field described by MM force field based on a free energy functional expressed by eq S2 (Supporting Information). The free energy functional represents a free energy surface defined by thermal distribution of the MM coordinates of the surrounding protein sampled by MD simulations. Geometry optimizations of the QM molecules searching the minimum and saddle points on the free energy surface are performed with the gradients of the free energy functional with respect to the QM coordinates and Hessian matrixes computed by a finite differential scheme with them (see Supporting Information).

Update of the MM conformational distribution upon changes of the electronic wave function and the geometry of the QM coordinates during the geometry optimization is carried out by a reweighting scheme[29] (see Supporting Information), which avoid frequent MD samplings. The ensemble average with the reweighting scheme, however, happens to become invalid for limited MM conformational samples obtained by a MD simulation during the geometry optimization cycle.[23] Thus, the MM conformational distribution is renewed by MD simulations until the reweighting average comes to stay valid. The macro-iteration of the renewal of the MM conformational samples by MD simulations is called the sequential sampling.[25]

Since the MM conformational distribution that determines the optimal QM geometry by the geometry optimization covers only limited region of the configurational space of the MM coordinates around each of the free energy stationary points of reactant, product and transition states, free energy differences between those states cannot be evaluated by the QM/MM-RWFE-SCF geometry optimizations for those individual states. The free energy differences are therefore calculated by MD simulations with the Bennett acceptance ratio (BAR) method of free energy perturbation.[26,27] The free energy differences between states 1 and 2, $\Delta F_{QM/MM}$, is expressed as

$$\Delta F_{QM/MM} = \Delta E^{0}_{QM} + \Delta E_{ZPE} + \Delta F_{vib} + \Delta F_{QM\text{-}MM,MM} \quad (1)$$

where ΔE^{0}_{QM} is the energy difference of the expectation values of the gas electronic Hamiltonian part, ΔE_{ZPE} is the zero point energy difference of the QM part, ΔF_{vib} is a contribution of vibrational entropy obtained with harmonic vibrational frequencies of the QM part, and $\Delta F_{QM\text{-}MM,MM}$ is the free energy difference originating from the QM-MM interaction and the MM part. ΔE_{ZPE} and ΔF_{vib} were evaluated with a Hessian matrix of the QM part.[25] It is noted that the vibrational entropy contributions may include a larger error than the zero point energy difference as the former contribution is more sensitive to errors of low frequency modes in a large QM system than the latter. In order to calculate the last term by the BAR method, both of the QM geometry and charges are linearly divided with a parameter λ_i as

$$\mathbf{R}_i = \lambda_i \mathbf{R}_2 + (1 - \lambda_i)\mathbf{R}_1$$
$$\mathbf{q}_i = \lambda_i \mathbf{q}_2 + (1 - \lambda_i)\mathbf{q}_1 \quad (2)$$

We defined a free energy surface in terms of the QM coordinate by eq S2 (Supporting Information). In this definition, the QM coordinates are regarded as external parameters in a thermodynamic sense, and the geometry optimization on the free energy surface corresponds to search of the optimal external parameters. A single transition state structure can therefore be determined on the free energy surface defined by eq S2 (Supporting Information). It is noted that the transition state on the free energy surface is an approximation of a more rigorous definition of the ensemble-averaged transition states where microstates of the reaction saddle points in the configuration space of the QM and MM coordinates are ensemble-averaged. Examination of the latter is, however, practically not possible as one needs to determine the saddle points of the QM coordinates for all of the conformational samples of the MM coordinates in the ensemble average. On the other hand, the approximation introduced in the present approach enables one to identify a representative transition state structure on a very extensive free energy surface constructed with ample statistical samples of the MM conformations and thus to elucidate a possible role of protein flexibility in energetics of enzymatic catalysis.

Semantic Clarification: Preorganization, Reorganization, Energetics, and Dynamics. Since it has been pointed out that discussions on role of protein flexibility in enzymatic reactions have suffered from semantic problems,[8] we first clarify physical chemistry underlying words representing enzymatic catalysis and protein flexibility in this report. Enzymatic catalysis is fulfilled by modulation of the chemical states of the reaction substrate in the protein binding pocket. One can consider two possible mechanisms of enzyme for the modulation of the transition state, that is, preorganization and reorganization.[8] The preorganization furnishes the protein binding pocket in the enzyme−substrate complex, that is, in the reactant state of reaction, with conformation that stabilizes the transition state, and any particular conformational changes of protein are not involved during the catalytic reaction process. On the other hand, the reorganization is defined as conformational changes of the binding pocket that accompany the formation of the transition state and play a role in the reaction catalysis.

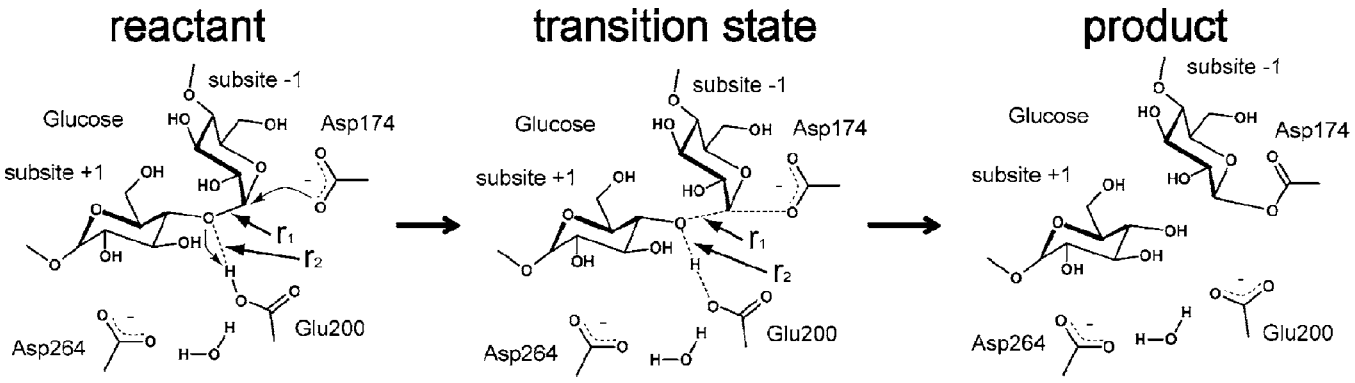

Figure 1. Reaction scheme of cleavage of the α-glycosidic bond in α-amylase catalysis studied in the present study. The product state corresponds to an intermediate of the overall α-amylase catalytic reaction proposed previously.[39] Numbers, +1 and −1, indicate the subsites of the substrate. The distance difference, $r_1 - r_2$, is used as the reaction coordinate.

The reorganization appears to be essential for electron transfer reactions in polar environments as revealed by Marcus theory.[28] Spontaneous conformational thermal fluctuation of the surrounding polar solvent molecules leads to the energy matching between the initial state and the final one that gives rise to the curve crossing between them. An energy associated with the reorganization, that is, the reorganization energy, determines energetics of the curve crossing process as predicted by Marcus's relation. In the case of enzyme, the reorganization can also alter energetics of the catalytic reaction as described below.

Since the reorganization is established by conformational changes of the surrounding environment, dynamics of the surrounding environment, in addition to the energetics described above, possibly affect the reaction catalysis. However, contribution of the dynamic effect depends on the time constant of reaction barrier crossing along the reaction coordinate, τ_{reac}, and of relaxation of the dynamics of the surrounding environment τ_{rlx}. When $\tau_{rlx} \ll \tau_{reac}$, thermal equilibrium in the reactant state is attained so that the reaction kinetics is well determined by the transition state theory and thus governed solely by energetics of the reaction free energy profile. On the other hand, in the case of $\tau_{reac} \ll \tau_{rlx}$, slow dynamics of the surrounding environment introduces deviation from kinetics of the transition state theory.

Let us now consider a catalytic reaction in the protein environment whose reaction free energy profile is schematically depicted in Figure 2. The reaction involves reorganization of the protein environment for the formation of the transition state which leads to reduction of free energy of the transition state. Assuming that vibrational relaxation along the local chemical reaction coordinates is fast and consequently equilibrium along the chemical reaction coordinates is always established, the reaction rate can varies in the range between k_{reorg} and k_{preorg} ($k_{reorg} > k_{preorg}$) depending on the time constants of τ_{reac} and τ_{rlx}. In the case of $\tau_{rlx} \ll \tau_{reac}$, the reaction trajectory proceeds through the transition state at the minimum free energy saddle point by the fast reorganization. As a result, the reaction rate in this case, k_{reorg}, represents the upper bound of the reaction rate for the free energy surface. On the other hand, as the relaxation of protein is slower, the reaction path deviates more from the minimum free energy one, and thus the activation barrier that the reaction trajectory crosses becomes higher. Finally, in the case of $\tau_{rlx} \gg \tau_{reac}$, that is, the reaction without the reorganization, the reaction rate, k_{preorg}, gives the lower bound since no energetic stabilization at the transition state by the reorganization is involved. The consideration above illustrates that the reorganization by conformational changes of the protein, which is often detected and expressed as protein dynamics, can alter the energetics of the catalytic reaction, and consequently can accelerate the catalytic reaction rate.

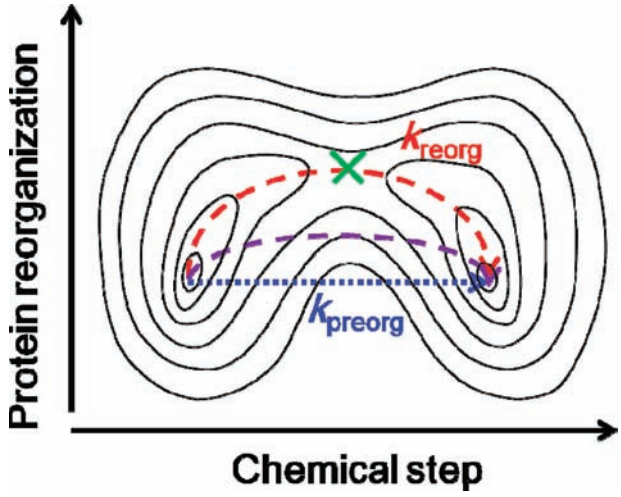

Figure 2. Free energy surface representing correlation between a chemical step and protein reorganization. Dashed lines indicate possible reaction paths and X indicates the transition state of the free energy surface. A reaction path drawn by a red line is the minimum free energy reaction path along which protein is reorganized completely. On the other hand, one by a blue line is a preorganization path without protein reorganization.

It has been pointed out[8] that reorganization is also involved in solution reactions and thus it is not a special mechanism of "enzymatic" catalysis. For solution reactions, linear response thermal fluctuation of solvents is mainly responsible for the reorganization as formulated in Marcus's theory. Obviously, such linear response fluctuation also exists in enzymes and contributes to the reorganization. However, in addition to the linear response fluctuation, proteins are known to exhibit characteristic nonlinear fluctuations involving large conformational changes, that is, transitions between conformational substrates,[2,29,30] which are absent in homogeneous solution systems. Hence, such nonlinear conformational transition can play a special role in catalysis of enzymes.

A characteristic of such nonlinear conformational transition is its slow relaxation behavior. In the case of linear response motion which comprise small atomic fluctuations or linear

dx.doi.org/10.1021/ja212117m | J. Am. Chem. Soc. 2012, 134, 7045−7055

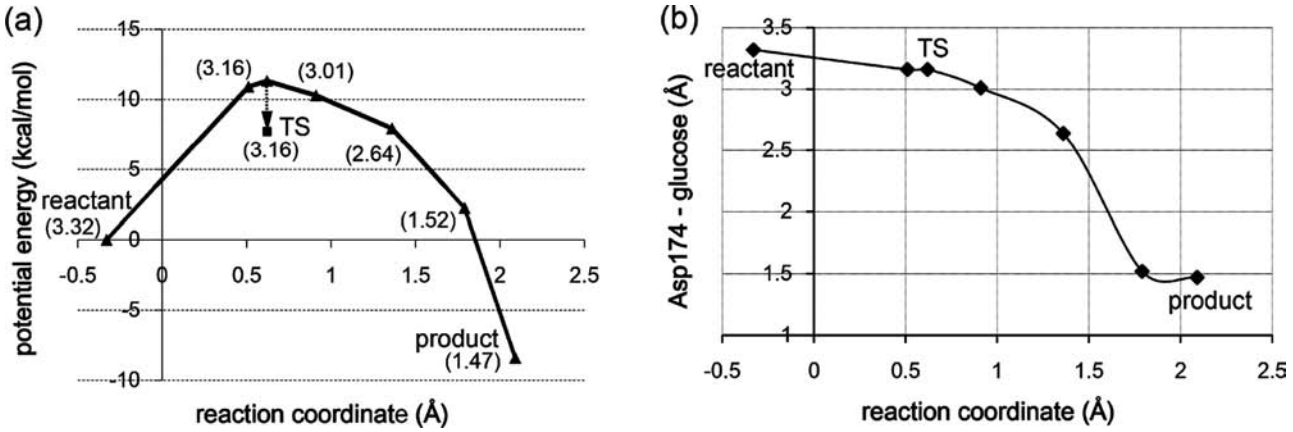

Figure 3. (a) QM/MM potential energy curve along the reaction coordinate (see Supporting Information). A structure at the barrier top of the potential energy curve was chosen for a starting point one of the saddle point search for the transition state determination after a low temperature MD equilibration of the MM part represented by a dotted arrow. Values in parentheses are distance between Asp174:O(6) and glucose:C(41) (see Figure S5, Supporting Information, for the atom index). (b) Change of distance between Asp174:O(6) and glucose:C(41) along the minimum energy path.

combinations of them, the relaxation time constant, τ_{rlx}, is typically in a range of sub picoseconds to tens of picoseconds. On the other hand, time scale of the nonlinear conformational relaxation is more than nanoseconds and can reach to milliseconds. Note here that, in spite of the slow relaxation time scale of the nonlinear conformational transition, the relaxation can be still faster than the reaction, that is, $\tau_{rlx} \ll \tau_{reac}$, and in turn the reorganization provides a significant contribution to the catalysis. Hence, in order to examine a possible role of the characteristic protein reorganization due to nonlinear conformational relaxation in enzymatic catalysis, a longer MD simulation capable of describing the nonlinear conformational relaxation is prerequisite. The present study aims at elucidating the energetics of the protein catalysis by the reorganization of the nonlinear conformational changes through a recently developed QM/MM method which permits one to describe slow nonlinear conformational changes of protein accompanied by the enzymatic reaction step.

COMPUTATIONAL DETAILS

The initial protein structure of α-amylase was taken from PDB 1G94,[31] which is of the protein with a saccharide substrate analog compound which occupies subsites −4 to +3. The substrate analog was replaced with an amylose which consists of six α-glucoses in subsites −4 to +2. The AMBER9 software suite[32] was used for all MD simulations. We employed the standard protonation states for titratable groups of the protein except for Glu200 being protonated, which were shown to be reasonable by pK_a calculations with PROPKA[33−36] (see Supporting Information). The QM/MM methods were implemented in GAMESS program package.[37] The QM region in the QM/MM calculations (Figure S1 in Supporting Information) treated by DFT/B3LYP with 6-31G* basis set except for the carboxyl groups of Asp and Glu, where the 6-31+G* basis set was employed, includes 69 atoms and the number of basis function is 629. Details of the QM/MM calculations are described in Supporting Information.

Before performing the QM/MM-RWFE-SCF geometry optimization on free energy surface, we carried out conventional QM/MM geometry optimizations on potential energy surface for a sphere cluster system (see Supporting Information) to obtain initial QM coordinates and charges for the free energy geometry optimization. The QM/MM-RWFE-SCF geometry optimizations and MD simulations for sampling of the MM conformational ensembles used in the geometry optimization were performed for a periodic boundary condition system where the protein-amylose complex is immersed in water solvent and sodium ions are added for charge neutralization (see Supporting Information) The total number of atoms of the system is 68533. ES interaction in the simulation box is fully taken into account with techniques based on the Ewald-summation method.[23] A 3-ns MD trajectory at 283 K was calculated at each macro-iteration step of the sequential sampling, and the first 1-ns and the last 2-ns trajectories were employed for equilibration and the sampling of the MM ensemble, respectively. The MM conformational samples were taken at every 100 fs, and thus the MM ensemble at each step of the sequential sampling was comprised of 20000 conformational samples. We confirmed that the stationary geometry of the product state on the free energy surface determined with MM samples obtained by a MD simulation for 2 ns stays essentially the same after the free energy geometry optimization with MM samples of an extended MD simulation for 10 ns. It is therefore considered that the stationary points obtained by the present protocol of free energy geometry optimization are stable free energy minima.

RESULT AND DISCUSSION

QM/MM Determination of the Reaction Transition State on a Potential Energy Surface. First, a potential energy curve along the reaction coordinate, $r = r_1 - r_2$, defined in Figure 1 was obtained by QM/MM potential energy geometry optimizations for the sphere cluster system (see Supporting Information for details of calculation protocols). Figure 3a displays the potential energy curve of the reaction. A potential energy barrier appears in rearrangement of chemical bonds at the α-glycosidic oxygen, (r = 0.62 Å), that is, proton transfer from Glu200 to the α-glycosidic oxygen and breakage of the α-glycosidic bond, although the potential energy profile in the region after the barrier top where attack of Asp174 takes place is very flat. Figure 3b shows that the attack of Asp174 proceeds spontaneously along the reaction coordinate which do not even represent the attack of Asp174. The transition state at the barrier top therefore constitutes the main activation barrier for the reaction. Although a decisive determination of the reaction mechanism may require a two-dimensional potential energy surface calculation in terms of the reaction coordinate r and a distance representing the attack of Asp174, such a detailed examination is beyond the scope of the present study. After an equilibration by MD simulation of the MM part at a low temperature (50 K) to remove a possible trap at a local minimum with a shallow well, the saddle point was searched from the geometry at the barrier top. The transition state

dx.doi.org/10.1021/ja212117m | J. Am. Chem. Soc. 2012, 134, 7045−7055

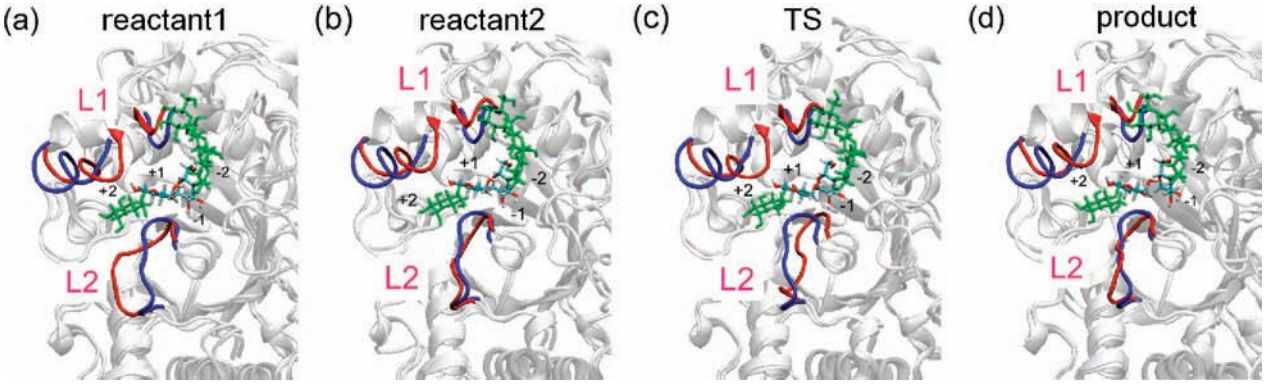

Figure 4. Conformational changes of the protein loops, L1 and L2, adjacent to the substrate binding site observed in the free energy geometry optimizations. The loops undergo large conformational transitions from the initial MM structure obtained by the QM/MM potential energy geometry optimization (blue) to the final structure of the free energy geometry optimization (red) in the (a) reactant1, (b) reactant2, (c) transition state and (d) product state. Reweighted average structures are shown for the free energetically optimized ones. The substrates are depicted in licorice representation, and their QM and MM regions are drawn in colors based on the atom type and in green, respectively. Numbers, −2 to +2, are the subsite indices of the substrate.

determined was confirmed to have one imaginary frequency ($104.15i$ cm^{-1}) by a calculation of Hessian matrix.

QM/MM Determination of the Reaction Transition State on a Free Energy Surface. By using the transition state on the QM/MM potential energy surface as the initial state for the QM/MM-RWFE-SCF calculation, we searched the transition state of the active site that includes the reactive moiety of the substrate molecule and the surrounding amino acid side chains for the chemical reaction depicted in Figure 1 on free energy surface defined by thermal distribution of the surrounding protein environment (see Theoretical Background, Computational Detail, and Supporting Information for methodological and computational details). First, in order to obtain a geometry proximal to the transition state on the free energy surface, we carried out a free energy minimization from the starting geometry where the reaction coordinate, r, is fixed. As shown in Figure S2 in Supporting Information, the free energy optimization is finished at 11th step of the sequential sampling (see Theoretical Background), that is, 33 ns MD simulations in total. The reweighted MM ensemble provides a well weighted ensemble average. Throughout the following transition state search and Hessian matrix calculations on free energy surface, the MM conformational samples at the last step of the sequential sampling were employed.

A transition state search on free energy surface from the free energetically optimized geometry described above with a free energy Hessian matrix successfully found the transition state. One of vibrational frequencies of normal modes on free energy surface at the transition state was confirmed to be imaginary, $178.61i$ cm^{-1}. As shown in Figure S3 in Supporting Information, the imaginary mode aligns well along the reaction coordinate, corroborating the validity of the transition state geometry. As the free energy optimization with the fixed reaction coordinate seen above provided a good starting point structure for the subsequent saddle point search for the transition state geometry determination, the QM geometry did not change largely by the transition state search. Consequently, the reweighted MM ensemble still provides well weighted ensemble average for the transition state as shown in Figure S2. A sequential sampling for the transition state search was therefore omitted.

Protein Conformational Changes during the Catalytic Reaction. Figure 4 displays the conformational changes of protein found in the QM/MM-RWFE-SCF geometry optimizations. The loop conformations shown in Figure 4 were obtained by reweighted averages over the MM samples of the last steps of the sequential samplings of the geometry optimizations. The conformational changes in the reactant1 and product states were reported previously.[23] The protein loops around the binding site, that is, L1 and L2, underwent large conformational changes. As shown in Figure S4, Supporting Information, large conformational changes are also observed at the L3 loop which is located far from the binding site but can interact with the L2 loop (see below). Interestingly, the conformations of the L2 loop in the optimized structures differ considerably among the chemical states of the enzymatic reaction. The L2 loop in the reactant1 state (Figure 4a) is unwound and extended toward the subsite +1 and consequently forms interaction with it, whereas the L2 loops in the transition (Figure 4c) and product (Figure 4d) states stay compact and thus lack the interaction. The L2 loop includes many glycine residues which furnish the loop with the high flexibility. The striking conformational difference of the L2 loop made us suspect that a local free energy minimum of a reactant state with a compact form of the L2 loop may exist. We found such a reactant state, the reactant2 (Figure 4b), by a free energy geometry optimization with 11 steps of the sequential sampling, that is, 33 ns MD simulation in total, from a starting geometry where the reactant QM structure is inserted into the product protein one. The conformational changes of the L2 loop shown in Figure 4 suggest that the conformational substates of the reactant1 and the reactant2 are in equilibrium and the chemical reaction proceeds from the reactant2 state. Unfortunately, examination of the transition between the conformational substates of the reactant1 and the reactant2 and a barrier crossing process proceeding directly from the reactant1 requires computationally very demanding molecular simulations. We therefore leave them in a future study.

Formation of the Reaction Transition State Accompanying Protein Reorganization. In the present study, we focus on the reaction process from the reactant2 state as the L2 loop in the reactant2 forms in a conformation more similar to that in the product state as observed in the optimized structures (Figure 4). Although the L2 loop keeps a compact form during the reaction process from the reactant2 state, it moves significantly upon the free energy reaction barrier crossing. As

dx.doi.org/10.1021/ja212117m | J. Am. Chem. Soc. 2012, 134, 7045−7055

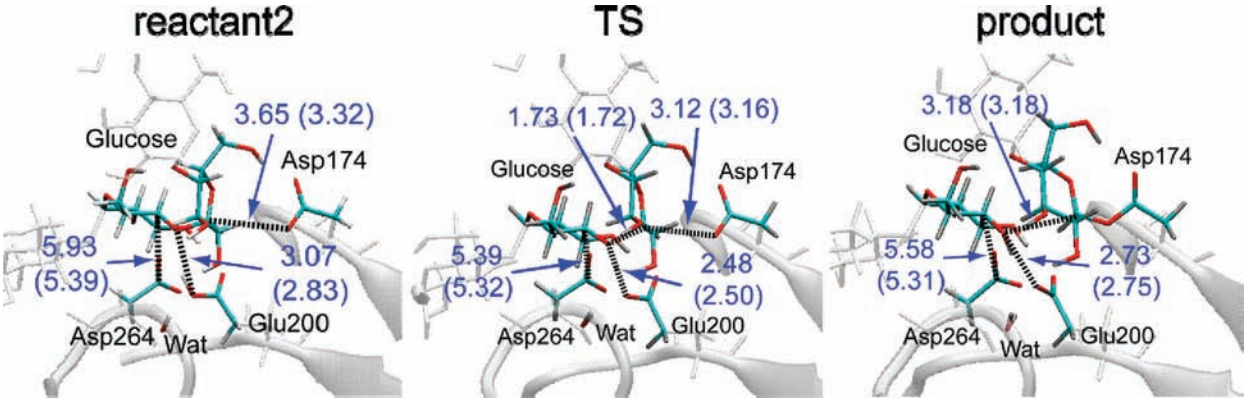

Figure 5. Changes of the QM geometries obtained by the QM/MM free energy optimizations. Left, middle and right panels depict the free energetically optimized QM structures in the reactant2, the transition state and the product, respectively. Distances between Asp174:O(6) and glucose:C(41) for the reactant, glucose:O(40) and glucose:C(41) for the product, Glu200:O(12) and glucose:O(40), and Asp264:C(17) and glucose:C(30) are shown (see Figure S5 for the atom index). The distances in parentheses are ones for the QM/MM structures determined by the QM/MM potential energy geometry optimization.

seen in Figure 4, the L2 loop approaches more closely to the catalytic core region around the junction between the subsites +1 and −1 at the transition state than at the reactant2 and product states. The movement manifests a large reorganization of the adjacent protein loop coupled with the chemical reaction. The conformational change of the main chain of the loop by ∼1.45 Å is much larger than its root-mean-square fluctuations (∼0.73 Å), indicating that the movement of the reorganization exceeds thermal fluctuation in a linear response regime and thus cannot be detected by a shorter MD simulation on a time scale less than nanoseconds. In fact, as seen below, relaxation of the conformational change is considerably slow.

The optimized QM structures of the catalytic site are shown in Figure 5. In the reactant2 state where strong intermolecular interactions are absent, thermal fluctuation of the protein environment taken into account in the free energy geometry optimization elongates hydrogen-bond distances in the catalytic region. As contrary, strong electronic interactions developing over the catalytic core region in the transition state are kept or even slightly enhanced by the thermal reorganization of the protein environment. For example, the intermolecular distances between the substrate, Asp174 and Glu200 become shorter than those optimized on the potential energy surface, 3.16 → 3.12 Å and 2.50 → 2.48 Å, respectively. The tendency regarding the strong electronic interactions is also observed in the product state.[23]

Figure 6 illustrates how the large conformational movement of the L2 loop shown in Figure 4 is induced by the local geometrical change of the chemical reaction. As seen in Figure 5, the prominent decrease of the distance between the glycosidic oxygen atom, O(40), and the O(12) atom of Glu200 (the numbers in parentheses are the atom indices defined in Figure S5, Supporting Information) by 0.59 Å accompanied by a proton transfer between them characterizes the transition state geometry. The movement of Glu200 propagates to Asp264 via a water molecule bridging between those carboxyl side chains and pull them toward the substrate. The remarkable decrease of the distance between Asp264:C(17) and glucose:C(30) upon the transition state formation (5.93 → 5.39 Å) shown in Figure 5 is a consequence of the movement of Asp264. Asn262 is also moved toward the substrate as its side chain is hydrogen-bonded with the bridging water molecule. As a result, the L2 loop which locates in a

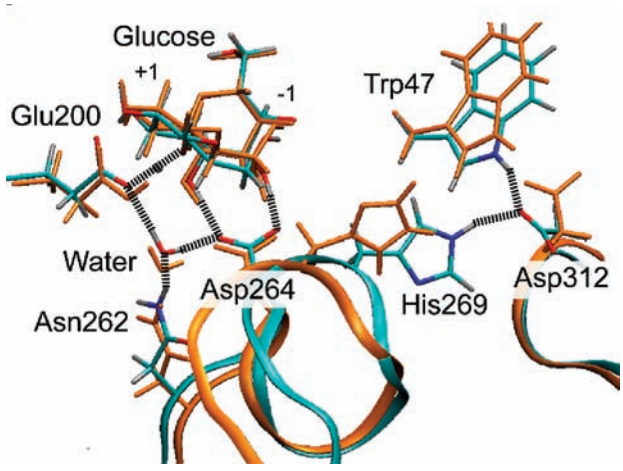

Figure 6. Important residues responsible for the L2 loop change between the reactant2 and the transition state. The residues of the reactant2 and the transition state are drawn in orange and in colors based on the atom type, respectively. Numbers, −1 and +1, are the subsite indices of the substrate. His269 included in the L2 loop forms a hydrogen-bond with Asp312 in the L3 loop (see Figure S4, Supporting Information) in the transition state.

sequentially neighbor region of Asn262 and Asp264 approaches to the substrate. The movement of the L2 loop is then amplified and stabilized by a newly formed hydrogen-bond between His269 and Asp312 which reside in the L2 and L3 loops, respectively.

Free Energy Profile of the Catalytic Reaction. We examined free energy profile of the reaction from the reactant2 state. The free energy differences, $\Delta F_{\mathrm{QM\text{-}MM,MM}}$, in eq 1 between the chemical states are calculated by the BAR method of free energy perturbation[26,27] (see Theoretical Background). The step size of the parameter, λ_i, in eq 2 was set to be 0.05, that is, the number of steps between the chemical states is 20. The step size was confirmed to be small enough to provide converged results (see Table S2 in Supporting Information).

First, a free energy difference at each step was computed with 10000 MM conformational samples obtained by a 1 ns trajectory after 1 ns equilibration. It is noted that the relaxation and sampling trajectory at each step is already one ∼3 orders of magnitude longer than that employed in free energy

dx.doi.org/10.1021/ja212117m | J. Am. Chem. Soc. 2012, 134, 7045−7055

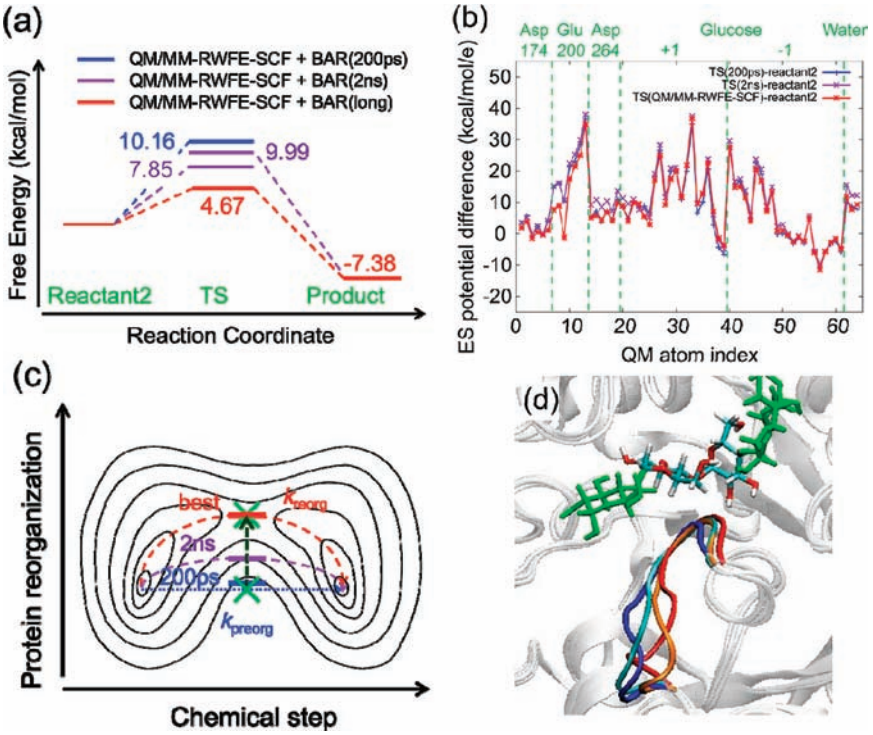

Figure 7. (a) Reaction free energy $\Delta F_{QM/MM}$ evaluated by eq 1 with the QM/MM-RWFE-SCF calculations and the MD simulations with the BAR method. The reaction free energies evaluated with shorter equilibrium MD ensemble sets (200 ps:100 ps equilibration and 100 ps sampling, and 2 ns:1 ns equilibration and 1 ns sampling, respectively) obtained by the forward MD samplings from the reactant2 and the product toward the transition state, respectively, for the BAR free energy calculations are also shown. (b) Differences in mean field ES potentials acting on the QM atoms between the reactant2 and the transition state. Differences between the ES potentials of the reactant2 and those evaluated by shorter relaxation simulations are also shown. For the latter simulations, sets of MM ensemble were obtained by the shorter MD simulations starting from the protein structure of the reactant2 with the QM geometry and charges of the transition state. (c) Diagram representing dependence of the activation free energy on the relaxation time of reorganization in the free energy evaluation. A reaction path deviates from the minimum free energy path from the reactant2 state as relaxations of the protein reorganization for 200 ps and 2 ns are not sufficient. A black dotted arrow represents schematically spontaneous relaxation observed in the nonequilibrium MD simulation from a starting structure where the QM structure and charges of the transition state were embedded in the protein structure of the reactant2 state. (d) Conformational transition of the L2 loop during the relaxation simulation starting from the protein structure of the reactant2 with the QM geometry and charges of the transition state. Average conformations of the reactant2 (blue), the first 1 ns MD ensemble of the relaxation after 1 ns equilibration (cyan), the last 1 ns MD ensemble of the relaxation for 11 ns (orange), and the transition state (red) are shown. The substrates are depicted in licorice representation, and their QM and MM regions are drawn in colors based on the atom type and in green, respectively.

calculations by direct QM/MM MD simulations reported thus far. The sets of the MM ensemble sampled in the free energy evaluation were generated from the MM conformations obtained at the last step of the sequential samplings of the QM/MM free energy geometry optimizations described above. To assess statistical convergence of the MM conformational samples, we tested the forward and backward sets of the samples which were generated by the MD simulations from the protein structures of the starting and end states, respectively. The errors, which are defined as deviations of the forward and backward sets from their mean, were found to be ±3.46 and ±4.19 kcal/mol for the free energy differences between the reactant2 and the transition states, and the transition state and the product, respectively (Table S2, Supporting Information). The relatively large errors, in spite of the longer equilibrium and sampling trajectories, originate from the lack of large conformational changes of the L2 loop which exhibit slow relaxation (see below). Note that the QM/MM geometry optimizations on free energy surfaces required ∼30 ns MD simulations where the large conformational changes of the adjacent loops are involved (Figure 4).

We therefore improved the statistical sampling by longer MD simulations. Since a longer MD simulation is needed as the step proceeds, we increased the simulation time for equilibration, T_i, in proportion to increment of the step as $T_i = 0.5\ \text{ns} \times (i - 1) + 1.0\ \text{ns}$ and $T_i = 0.5\ \text{ns} \times i + 1.0\ \text{ns}$ for odd and even i, respectively. Accordingly, MD equilibration times at the end point and in total for the forward and backward sets between the three chemical states were 11 and 484 ns, respectively. Although the errors were reduced to be 2.40 and 2.51 kcal/mol (Table S2, Supporting Information), respectively, they still remain considerable, indicating that the equilibration is still not sufficient. On the other hand, the averages of the free energy differences of the forward and backward sets and the differences evaluated by the BAR calculation with the ensemble set where the forward and backward ones are mixed do not largely differ for the shorter and longer equilibrations as seen in Table S2. Thus, those averaged free energy differences are expected to be less sensitive to the equilibration time due to cancellation of errors. Hereafter, the values of the BAR calculations with the mixed ensemble sets are employed for discussion.

As seen above, statistical convergence of the MM conformational samples becomes a critical problem when the large

dx.doi.org/10.1021/ja212117m | J. Am. Chem. Soc. 2012, 134, 7045−7055

Table 1. Components of the Energy Difference between the Chemical States in Equation 1 and Those of QM/MM Calculations on Potential Energy Surface[a]

TS − reactant2 (kcal/mol)	ΔE_{QM}	ΔE_{zero}	ΔF_{VIB}	$\Delta F_{QM\text{-}MM,MM}$	$\Delta E_{QM\text{-}MM}$	ΔE_{MM}	total
QM/MM[b]	7.59	−2.81	0.20		3.31	−3.18	5.11
QM/MM-RWFE-SCF	7.37	−3.29	1.25	−0.66	(−1.60)[c]		4.67
product − reactant2 (kcal/mol)	ΔE_{QM}	ΔE_{zero}		$\Delta F_{QM\text{-}MM,MM}$	$\Delta E_{QM\text{-}MM}$	ΔE_{MM}	total
QM/MM[b]	−11.61	−0.55	−0.38		5.57	−2.36	−9.33
QM/MM-RWFE-SCF	−11.13	0.39	−0.46	3.82	(−10.03)[c]		−7.38

[a]Expectation values of the gas Hamiltonian (ΔE_{QM}), zero point energies of the QM part (ΔE_{zero}), contributions of harmonic vibrational entropy of the QM part (ΔF_{vib}), free energies obtained by BAR calculations ($\Delta F_{QM\text{-}MM,MM}$), QM-MM interaction energies ($\Delta E_{QM\text{-}MM}$), MM energies (ΔE_{MM}), and total energies (total). [b]QM/MM calculations on potential energy surface. [c]Difference between reweighted averages of the QM-MM interaction energy.

protein conformational changes are correlated with the chemical reaction as found in the present study. Development of a more efficient sampling method would be necessary in a future study. The problem is that the MM ensembles in the free energy evaluation are not sufficiently relaxed with respect to changes of the QM structures and charges during the free energy evaluation due to limited relaxation time of the MD simulation. Although, according to a thermodynamic principle, free energy differences between two states are independent of a route connecting them, the straight interpolation between two states defined by eq 2 gives a high free energy path, which may disturb relaxation of the protein conformation. This possible problem could be alleviated by a free energy reaction path calculation[25,38] that searches a free energetically optimal route to connect two states and thus may enhance relaxation of the protein conformation. However, the reaction path search requires the QM/MM free energy geometry optimization at each dividing points along the path, whereas only classical MD simulations are needed in the free energy calculation in the present protocol. As the QM free energy optimization introduces costs approximately twice as much as the classical MD simulation for the present system in terms of computational time, we leave its development and application in a future study. Application of a path sampling method for the MM part exhibiting the protein conformational changes is also expected to accelerate the relaxation of protein drastically.

Figure 7a illustrates the reaction free energy profile of $\Delta F_{QM/MM}$ given by eq 1. The reaction barrier height and the reaction energy were evaluated to be 4.67 and −7.38 kcal/mol, respectively. Although the barrier height is comparable to that obtained by the QM/MM geometry optimization on the potential energy surface by 5.11 kcal/mol (Table 1), the accordance is accidental. Difference between the QM/MM calculation on the potential energy surface and that on the free energy surface comes from slow thermal relaxation of the surrounding protein environment on the tens of the nanoseconds time scale which is lack in the former. For the reactant2 state, as shown in Figure 5, largely elongated hydrogen-bonds in the catalytic region were observed as described above. The conformational changes of the catalytic region resulting from thermal relaxation of the surrounding protein environment imply large free energetic stabilization. For the transition state, slow thermal relaxation involving the L2 loop conformational changes observed is responsible for reduction of free energy of the transition state, which cancels the stabilization at the reactant2 state to some extent. A large decrease of the QM-MM interaction energy on free energy surface from its corresponding value on potential energy surface by −4.91 kcal/mol (Table 1) also implies significance of thermal reorganization of the catalytic binding site by protein relaxation. The view is corroborated by a large difference in ES potential acting on the QM atoms between the reactant2 and the transition state, that is, the reorganizing ES potential (Figure 7b). In particular, a large positive ES potential developing on an oxygen atom of a carboxyl group of Glu200 (the atom index 11 defined in Supporting Information) stabilizes the transition state because the carboxyl group becomes negatively charged as the reaction proceeds (Figure 1). The ES reorganization is considered to originate mainly from ES interaction of a neighboring group, Arg172, and a hydrogen-bond of a water molecule. Although other large reorganizing ES potentials are seen in Figure 7b, unfortunately, it is difficult to interpret those reorganizations on a molecular basis as they come from sums of contributions of various groups. As seen in Figure S6 (Supporting Information), the catalytic ES potential is considerably smaller in the potential energy geometry optimizations where the reorganization is drastically suppressed. The large thermal reorganization is also observed for the product state (Table 1 and Figure S6).

Role of the Slow Protein Reorganization in the Reaction Catalysis. To examine how the protein reorganization influences energetics of the chemical reaction, we evaluated the activation free energy barrier by the BAR method with conformational samples of the protein obtained by MD simulations for 200 ps, equilibration for 100 ps and sampling for 100 ps, at each dividing point from the reactant2 conformation. The relaxation for 200 ps along change of the substrate to the transition state, which is a typical time scale that conventional QM/MM MD simulations can cover, is much shorter than that observed for the conformational changes of the L2 loop on the tens of nanoseconds time scale. Thus, the activation free energy barrier obtained by the MD trajectories for 200 ps does not include most of the protein reorganization identified by the QM/MM free energy geometry optimization. As shown in Figure 7a, the activation barrier was evaluated to be 10.16 kcal/mol and thus is considerably higher than the best estimation of the barrier by much longer MD simulations, 4.67 kcal/mol. Doubling dividing points of the BAR calculations did not largely alter the activation energy (see Supporting Information), confirming that the increase of the activation free energy does not originate from an artifact the free energy perturbation scheme. The increase of the activation barrier by the lack of the sufficient relaxation of the protein reorganization is schematically illustrated in Figure 7c. The time constant of the chemical reaction, $\tau_{reac} = k_{reac}^{-1}$, for the 200-ps relaxation was estimated to be 13.8 μs by the transition state theory,

$$k_{reac} = \frac{k_b T}{h} \exp\left[-\frac{\Delta F^*}{k_b T}\right] \quad (3)$$

where ΔF^* is the activation free energy and h is the Planck constant. The time constant of the chemical reaction, τ_{reac}, is much longer than that of relaxation of the protein reorganization, τ_{rlx}, which is on the tens of nanoseconds time scale estimated from time scales observed in the QM/MM free energy geometry optimizations seen above and a MD simulation for the relaxation at the transition state described below. The protein reorganization is therefore expected to play a role in enhancing the chemical reaction rate by reducing the activation barrier as described above (see Theoretical Background). The protein conformational changes shown in Figure 6 are not those induced by the chemical reaction but are those facilitating the chemical reaction.

The activation free energy barrier evaluated with MD trajectories for 2 ns, which is much longer than 200 ps but is still shorter than the relaxation of the reorganization, was evaluated to be 7.85 kcal/mol as described above. The activation barrier is reduced by the longer relaxation for 2 ns, as schematically depicted in Figure 7c, but is still considerably higher by 3.18 kcal/mol than the best estimate. The relaxation for 2 ns is therefore not sufficient to attain the fully relaxed reorganization. The time constant of the chemical reaction is calculated to be 220 ns by the transition state theory, which is still longer than that of the relaxation of the reorganization.

The time constant of the chemical reaction for the best estimated activation barrier, 4.67 kcal/mol, is evaluated to be 0.735 ns, and thus is now shorter than that of the relaxation of the reorganization. Considering computational ambiguity of the reaction barrier calculation regarding accuracy of the methodology employed and assignment of protonation states of carboxylate in the catalytic site (see Supporting Information), it is concluded that the time constant of the chemical reaction is comparable to that of the protein reorganization involving the large conformational changes of the L2 loop. Thus, the reaction kinetics is energetically influenced by the slow protein reorganization on the tens of nanoseconds time scale; the chemical reaction is catalyzed by reduction of the activation barrier due to the slow protein reorganization. Although those time constants are estimated to be on the same order and thus explicit dynamic coupling between those phenomena may be involved, such a dynamic effect is out of the scope of the present study.

The view above is supported by the conformational changes of the L2 loop observed in a MD simulation of the protein relaxation upon the instantaneous change of the chemical states. In this simulation, a nonequilibrium trajectory calculation was carried out from a starting structure where the QM structure and charges of the transition state were embedded in the protein structure of the reactant2 state. The MD simulation therefore represents protein relaxation from a free energetically unstable state as schematically illustrated in Figure 7c. The conformational changes of the L2 loop during the relaxation are shown in Figure 7d. A half of the L2 loop proximal to the catalytic core approaches to it already in the first 2 ns of the protein relaxation. The other half far from the catalytic core stays in a conformation closer to that of the reactant2 in the first 2 ns, and it moves gradually toward a conformation of the transition state in the following relaxation for 9 ns. The spontaneous relaxation of the loop conformation toward that of the transition state indicates that the chemical transition state is free energetically more stable in the transition state loop conformation obtained through the protein reorganization. The complete conformational changes of the L2 loop is expected to be achieved by the formation of a hydrogen-bond between His269 and Asp312 described above, which does not take place yet in the relaxation for 11 ns. As seen above, the conformational changes of the L2 loop proceeds to some extent without formation of the hydrogen-bond between His269 and Asp312. Thus, it is expected that the activation free energy is also reduced to some extent by similar conformational changes of the L2 loop without the hydrogen-bond, although the reduction of activation energy is smaller than that with the hydrogen-bond formation.

The spontaneous relaxation of the loop conformation was also observed for the reverse process, that is, the relaxation from the transition state protein structure toward the reactant2 one upon the replacement of the QM regions (Figure S7, Supporting Information). The conformation of the L2 loop is therefore well correlated with the chemical states of the catalytic reaction site.

A catalytic role of the correlation between the local movement at the reaction core and the large conformational changes of the L2 loop upon the formation of the transition state may be demonstrated more directly by examination of the reaction free energy profile for site-specific mutants where a hydrogen-bond between the reaction core and the L2 loop is disrupted. Unfortunately, however, such examination is not an easy task. First, as shown in the present study, accurate evaluation of the reaction free energy profile requires very demanding computation due to the nature of the slow protein conformational changes. Second, it is highly expected that such disruption of a hydrogen-bond to a loop region leads to large deformation or unfolding of its conformation, making interpretation of the result very difficult. Because of the difficulties above, we leave such examination in a future study.

A question now arises; how do the local changes of the structure and the charges at the reaction core during the chemical reaction correlate with the extended conformational changes of protein despite the difference in the spatial scale? It is unlikely that direct interaction of the L2 loop with the reaction core modulates strongly the energetics of the reaction process because of their large mutual distance. In order to analyze the interaction of the reaction core with the protein, the reorganizing ES potential difference of the free energetically optimized states is compared with those resulting from the shorter relaxations for 200 ps and 2 ns seen above. One can discern in Figure 7b that the protein relaxations within 200 ps and 2 ns upon the sudden changes of the chemical states produce reorganizing ES potentials closely similar to that obtained for the free energetically optimized state, respectively, indicating that the ES reorganization in the catalytic site is already established in a short time range before the large conformational changes of the L2 loop take place. The fast formation of the reorganizing ES potentials may represent a key feature of the catalysis of a preorganized structure of protein.

The ES reorganization can be produced by fast conformational fluctuation around the catalytic site, presumably in a linear response regime, which was simulated by the virtual nonequilibrium MD simulations of the protein response to the instantaneous change of the chemical states. As the ES reorganization is induced by ES response to the small changes of structure and partial charges of the reaction core, the ES response is considered to include mainly contributions from

interaction with the surrounding protein groups relatively near the reaction core. The local response in a short time range was observed in the nonequilibrium MD simulations of the protein response seen above (Figure 7d); the conformational changes of the L2 loop close to the reaction core occurs in a short time range, whereas the other half of the L2 loop remote from the reaction core exhibits slow relaxation. However, the fast local reorganization is not well accommodated in the global conformation of protein without the slow reorganization as observed for the L2 loop, and leads to a free energetically unstable transition state of the reaction giving rise to drastic reduction of the kinetic rate as seen above. The conflict is reconciled by the slow conformational movement of protein beyond the linear response regime that well accommodates and stabilizes the local reorganization. In the actual barrier crossing process, the fast local reorganization is slaved by the slow conformational fluctuation of protein because of the difference in the relaxation time scale. The local reorganization is therefore governed to some extent by the slow conformational fluctuation.

The insight into a role of the protein slow reorganization in the catalysis obtained above proposes a possible scenario that can explain a molecular mechanism underlying the phenomena of "dynamic knockout" reported recently.[9] In the dynamic knockout experiments, mutations that do not disturb the protein structure observed by X-ray crystallography but do suppress conformational flexibility measured by relaxation-dispersion NMR were observed to impair a chemical reaction of dihydrofolate reductase. The mechanism obtained in the present study demonstrates on a molecular basis that a slow protein reorganization by transition to a transiently formed conformational substate, which cannot be detected by crystallography but can be by relaxation-dispersion NMR, is able to reduce the activation barrier of reaction, and how such catalysis by correlation between a reaction step and slow protein reorganization is achieved.

CONCLUSION

The present study uncovered in an atomic detail a crucial role of the large and slow conformational changes of protein upon formation of the chemical transition state in the catalytic reaction on structural and energetics bases. Structural change of the reaction core in the transition state formation involving proton transfer was observed to correlate with the large conformational changes of the adjacent loop of protein on the tens of nanoseconds time scale. The chemical reaction was observed to be catalyzed by reduction of the activation free energy through stabilization of the transition state by protein reorganization involving the large and nonlinear conformational changes of protein. The transition state stabilization is attained in a way that local protein structural changes around the reaction core responsible for a fast (less than a nanosecond) reorganization to the change of the chemical state upon the formation of transition state is energetically stabilized by the slower and more extended conformational changes of protein.

A remaining question is dynamic aspect of the slow conformational changes in the kinetics of the catalytic reaction. Analysis based on a multidimensional free energy surface conceptually realized by Sumi-Marcus model[40] would provide an insight into the protein dynamics and the catalytic kinetics. The complete scheme of the glycosidic bond dissociation through examination of energetic and kinetic properties for transitions between the reactant substates, that is, the reactant1 and reactant2 states, and a barrier crossing directly proceeding from the reactant1 state also remains to be determined for definitive understanding of biochemical mechanism of the enzymatic process. Design of a reaction transition state by the present methodology together with experimental and computational design of conformational substates[41] will be a powerful approach for protein engineering of enzyme.

ASSOCIATED CONTENT

Supporting Information

Supplementary materials as noted in text. This material is available free of charge via the Internet at http://pubs.acs.org.

AUTHOR INFORMATION

Corresponding Author

*hayashig@kuchem.kyoto-u.ac.jp

Notes

The authors declare no competing financial interest.

ACKNOWLEDGMENTS

The study was supported by research fellowships for young scientist from the Japan Society for the Promotion of Science (JSPS) to T.K., by Grant-in-Aid for Scientific Research on Priority Areas (18074004) and that on Innovative Areas (23107717) from the Ministry of Education, Culture, Sports, Science, and Technology, Japan, by Grant-in-Aid for Scientific Research from JSPS (23700580), by Research and Development of the Next-Generation Integrated Simulation of Living Matter, and the Global COE program "International Center for Integrated Research and Advanced Education in Materials Science".

REFERENCES

(1) Wolf-Watz, M.; Thai, V.; Henzler-Wildman, K.; Hadjipavlou, G.; Eisenmesser, E. Z.; Kern, D. *Nat. Struct. Mol. Biol.* **2004**, *11*, 945−949.
(2) Boehr, D. D.; McElheny, D.; Dyson, H. J.; Wright, P. E. *Science* **2006**, *313*, 1638−1642.
(3) Watt, E. D.; Shimada, H.; Kovrigin, E. L.; Loria, J. P. *Proc. Natl. Acad. Sci. U.S.A.* **2007**, *104*, 11981−11986.
(4) Masterson, L. R.; Cheng, C.; Yu, T.; Tonelli, M.; Kornev, A.; Taylor, S. S.; Veglia, G. *Nat. Chem. Biol.* **2010**, *6*, 821−828.
(5) Masterson, L. R.; Shi, L.; Metcalfe, E.; Gao, J.; Taylor, S. S.; Veglia, G. *Proc. Nat. Acad. Sci. U.S.A.* **2011**, *108*, 6969−6974.
(6) Hammes-Schiffer, S.; Benkovic, S. J. *Annu. Rev. Biochem.* **2006**, *75*, 519−541.
(7) Nagel, Z. D.; Klinman, J. P. *Nat. Chem. Biol.* **2009**, *5*, 543−550.
(8) Kamerlin, S. C. L.; Warshel, A. *Proteins* **2010**, *78*, 1339−1375.
(9) Bhabha, G.; Lee, J.; Ekiert, D. C.; Gam, J.; Wilson, I. A.; Dyson, H. J.; Benkovic, S. J.; Wright, P. E. *Science* **2011**, *332*, 234−238.
(10) Warshel, A.; Levvit, M. *J. Mol. Biol.* **1976**, *103*, 227−229.
(11) Field, M. J.; Bash, P. A.; Karplus, M. *J. Comput. Chem.* **1990**, *11*, 700−733.
(12) Gao, J. *Acc. Chem. Res.* **1996**, *29*, 298−305.
(13) Svensson, M.; Humbel, S.; Froese, R. D. J.; Matsubara, T.; Sieber, S.; Morokuma, K. *J. Phys. Chem.* **1996**, *100*, 19357−19363.
(14) Monard, G.; Merz, K. M., Jr. *Acc. Chem. Res.* **1999**, *32*, 904−911.
(15) Yang, Y.; Yu, H.; Cui, Q. *J. Mol. Biol.* **2008**, *381*, 1407−1420.
(16) D'Amico, S.; Gerday, C.; Feller, G. *J. Biol. Chem.* **2001**, *276*, 25791−25796.
(17) D'Amico, S.; Gerday, C.; Feller, G. *J. Biol. Chem.* **2002**, *277*, 46110−46115.
(18) D'Amico, S.; Marx, J.-C.; Gerday, C.; Feller, G. *J. Biol. Chem.* **2003**, *278*, 7891−7896.
(19) Siddiqui, K. S.; Cavicchioli, R. *Annu. Rev. Biochem.* **2006**, *75*, 403−433.

(20) Spiwok, V.; Lipovová, P.; Skálová, T.; Dušková, J.; Dohnálek, J.; Hašek, J.; Russell, N. J.; Králová, B. *J. Mol. Model.* **2007**, *13*, 485−497.
(21) Pasi, M.; Riccardi, L.; Fantucci, P.; Gioia, L. D.; Papaleo, E. *J. Phys. Chem. B.* **2009**, *113*, 13585−13595.
(22) Kosugi, T.; Hayashi, S. *Chem. Phys. Lett.* **2011**, *501*, 517−522.
(23) Kosugi, T.; Hayashi, S. *J. Chem. Theory Comput.* **2012**, *8*, 322−334.
(24) Yamamoto, T. *J. Chem. Phys.* **2008**, *129*, 244104.
(25) Hu, H.; Lu, Z.; Parks, J. M.; Burger, S. K.; Yang, W. *J. Chem. Phys.* **2008**, *128*, 034105.
(26) Shirts, M. R.; Bair, E.; Hooker, G.; Pande, V. S. *Phys. Rev. Lett.* **2003**, *91*, 140601.
(27) Shirts, M. R.; Pande, V. S. *J. Chem. Phys.* **2005**, *122*, 144107.
(28) Marcus, R. A. *J. Chem. Phys.* **1956**, *24*, 966−978.
(29) Frauenfelder, H.; Parak, F.; Young, R. D. *Annu. Rev. Biophys. Biophys. Chem.* **1988**, *17*, 451−479.
(30) Shaw, D. E.; Maragakis, P.; Lindorff-Larsen, K.; Piana, S.; Dror, R. O.; Eastwood, M. P.; Bank, J. A.; Jumper, J. M.; Salmon, J. K.; Shan, Y.; Wriggers, W. *Science* **2010**, *330*, 341−346.
(31) Aghajari, N.; Roth, M.; Haser, R. *Biochemistry* **2002**, *41*, 4273−4280.
(32) Case, D. A.; Darden, T. A.; Cheatham, T. E., III; Simmerling, C. L.; Wang, J.; Duke, R. E.; Luo, R.; Merz, K. M.; Pearlman, D. A.; Crowley, M.; Walker, R. C.; Zhang, W.; Wang, B.; Hayik, S.; Roitberg, A.; Seabra, G.; Wong, K. F.; Paesani, F.; Wu, X.; Brozell, S.; Tsui, V.; Gohlke, H.; Yang, L.; Tan, C.; Mongan, J.; Hornak, V.; Cui, G.; Beroza, P.; Mathews, D. H.; Schafmeister, C.; Ross, W. S.; Kollman, P. A. *AMBER 9*; University of California: San Francisco, CA, 2006.
(33) Li, H.; Robertson, A. D.; Jensen, J. H. *Proteins* **2005**, *61*, 704−721.
(34) Bas, D. C.; Rogers, D. M.; Jensen, J. H. *Proteins* **2008**, *73*, 765−783.
(35) Olsson, M. H. M.; Søndergaard, C. R.; Rostkowski, M.; Jensen, J. H. *J. Chem. Theory Comput.* **2011**, *7*, 525−537.
(36) Søndergaard, C. R.; Olsson, M. H. M.; Rostkowski, M.; Jensen, J. H. *J. Chem. Theory Comput.* **2011**, *7*, 2284−2295.
(37) Schmidt, M. W.; Baldridge, K. K.; Boatz, J. A.; Elbert, S. T.; Gordon, M. S.; Jensen, J. H.; Koseki, S.; Matsunaga, N.; Nguyen, K. A.; Su, S.; Windus, T. L.; Dupuis, M.; Montgomery, J. A. *J. Comput. Chem.* **1993**, *14*, 1347−1363.
(38) Hu, H.; Lu, Z.; Yang, W. *J. Chem. Theory Comput.* **2007**, *3*, 390−406.
(39) Qian, M.; Nahoum, V.; Bonicel, J.; Bischoff, H.; Henrissat, B.; Payan, T. *Biochemistry* **2001**, *40*, 7700−7709.
(40) Sumi, H.; Marcus, R. A. *J. Chem. Phys.* **1986**, *84*, 4894.
(41) Bouvignies, G.; Vallurupalli, P.; Hansen, D. F.; Correia, B. E.; Lange, O.; Bah, A.; Vernon, R. M.; Dahlquist, F. W.; Baker, D.; Kay, L. E. *Nature* **2011**, *477*, 111−114.